OPTIMIZATION STRATEGIES FOR OPTIMUM POWER GENERATION IN PIEZOELECTRIC ENERGY HARVESTING FROM AMBIENT VIBRATIONS

Vitor Ramos Franco, vrfranco@sc.usp.br
Andreza Tangerino Mineto, andreza@sc.usp.br
Paulo Sérgio Varoto, varoto@sc.usp.br
Laboratory of Dynamics, USP/EESC–School of Engineering of Sao Carlos-USP, Ave.Trabalhador São-Carlense, 400, ZIP CODE 13566-590, São Carlos - SP – Brazil.

Abstract. *In the past recent years increasing research efforts have been dedicated to the issue of harvesting ambient structural vibration signals through piezoelectric materials. In this context the use of optimization techniques play an important role in the design of a given device since they often lead to a set of geometric parameters that will ultimately convey the best performance for the harvester in terms of the output electrical power. Hence, this article is focused in studying optimization techniques and their application to enhance the performance of piezoelectric energy harvesters composed by cantilever beam carrying a tip mass excited from base accelerations. Parameters as for example the length of the piezoelectric element, the length of the substructure and the value of the tip mass are adjusted by employing different optimization strategies in order to reach the optimum performance for the harvester in terms of power generation. Results from two different optimization techniques (Sequential Quadratic Programming, SQP, and Extensive Search, ES) were compared by using peak values from the electromechanical FRFs.*

Keywords*:Energy Harvesting, Optimization Techniques, SQP, FRF*

1. INTRODUCTION

Harvesting energy from environmental lost vibrations through the conversion of mechanical to electrical energy has been a topic of major interest in the last five years. Important contributors (Erturk et al., 2009a, Stanton et al., 2009) focused on different modeling strategies of energy harvesting systems by analyzing the effect of design parameters such as load resistance and electromechanical coupling coefficient (EMCC) on the device's capability of generating electrical power. For instance, Renno et al. (2009) provided an analysis of the effects of structural damping and electromechanical coupling on the optimal energy harvesting from a vibration source and the resulting cases were treated and examined by optimizing the circuit parameters in order to obtain the maximum electrical power. Bourisli et al. (2010) used genetic algorithms (GAs) to optimize the area covered by piezoelectric material of a shear deformable cantilever beam for maximum modal electromechanical coupling coefficient. In this work, the geometrical configuration of a PZT layer covering a beam is optimized for each of the first three modes to maximize the modal EMCC.

Additional investigations focused on the optimization of the circuit topologies or on the shape of the harvesters. One of the most efficient and simple optimization techniques is based on tuning both of the electrical and mechanical impedances (impedance matching) (Renno et al., 2009). Wickenheiser et al. (2010) studied the maximum power operating conditions for piezoelectric energy harvesters when connected to several different circuit topologies. According to the authors, the results enables the choice of the load impedance to maximize the power harvested depending on the characteristics of the energy harvesting system.

Based on the problem of obtaining the optimum electrical power limited by the shape of piezoelectric layer in a bimorph energy harvesting device, Dietl et al. (2010) proposed a new approach by changing the shape of the beam to concentrate the strain in sections of the beam where it can offer the maximum contribution in terms of mechanical to electrical energy transduction. Three beams with different shapes were tested over a wide band, encompassing the lowest two modes of vibration. Optimal beams were found to improve the power transduction from sinusoidal base excitation to electrical power.

In this paper, the Sequential Quadratic Programming (SQP) method was used to optimize some parameters of the energy harvesting device for obtaining the maximum output power. Results of this approach are compared to a proposed optimization methodology based on the variation of geometrical parameters of the harvesting device in order to obtain the best configuration that maximizes the peak voltage in the FRF. The techniques were numerically applied in a bimorph cantilever beam with tip mass submitted to its base translation in its first natural frequency.

2. ELECTROMECHANICAL MODEL OF THE CANTILEVER BIMORPH PIEZOELETRIC HARVESTER

This section describes the electromechanical model of the cantilever harvester used in the numerical simulations. The mode is based on the work by Erturk (Erturk et al, 2009a, b) except that in the present case it is assumed that the substrate beam is partially covered by the piezoelectric material thus forming a segmented piezoelectric device. This segmented harvesting configuration is necessary in this case since one of the major goals of the optimization technique is to find the optimum solution for the length of the piezo layer.

The harvester consists of a cantilever beam with segmented piezoelectric layers covering the top and bottom surfaces (bimorph configuration) and a tip mass. The harvester was submitted to a base acceleration composed by transversal and rotational motions. As suggested by Timoshenko et al. (cited by Erturk et al. 2009a,b) the absolute transverse motion of the beam at any point (x) and time (t) can be written as

$$u(x,t)=u_b(x,t)+u_{rel}(x,t) \tag{1}$$

where $u(x,t)$ is the absolute transverse motion of the beam, $u_b(x,t)$ is the transverse motion of the base and $u_{rel}(x,t)$ is the curvature of the beam. The transverse motion of the base, $u_b(x,t)$, can be written as

$$u_b(x,t)=g(t)+xh(t) \tag{2}$$

where $g(t)$ and $h(t)$ are the translational and rotational components respectively. In this study, the rotational component of the input motion will be neglected.

The configuration of the harvester is shown in Fig. (1a) and the cross sectionals A-A and B-B are shown in Fig. (1b).

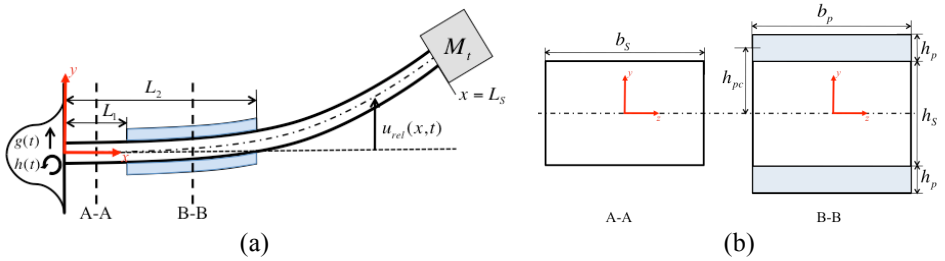

Figure 1. (a) Bimorph cantilever beam used as an Energy Harvesting system; (b) cross sectionals A-A and B-B.

It is known in the circuitry-based energy harvesting literature that a piezoelectric element can be represented as a current source in parallel with its internal capacitance (Erturk et al., 2009b). Thus, the energy harvesting system showed in Fig. (1a) can be represented by a simple circuit in series connection of the piezo layers as shown in Fig. (2).

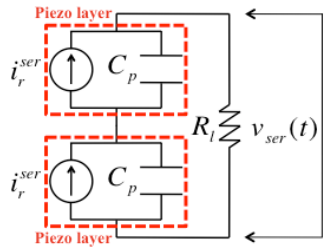

Figure 2. Electrical circuit representing the series connection of the piezo layers

In Fig. (2), R_l is the resistive load connected to the piezo layers, i_p^{ser} is the current source and C_p is the internal capacitance of the piezoelectric element which is given by

$$C_p=\frac{\bar{\varepsilon}_{33}^S b_p L_p}{h_p} \tag{3}$$

where ε_{33}^{S} is the permittivity component at constant stress, b_p is the width of the piezo, L_p is the length of the piezo and h_p is the thickness of the piezo.

Assuming the well known proportional damping assumption, the vibration response relative to the base of the bimorph can be represented as an absolutely and uniform convergent series of the eigenfunctions for the series connection of the piezo layers as (McConnell et al. 2008)

$$u_{rel}^{ser}(x,t) = \sum_{r=1}^{\infty} U_r(x)\eta_r^{ser}(t) \tag{4}$$

where $U_r(x)$ is the mass normalized eigenfunction of the r^{th} vibration mode, $\eta_r^{ser}(t)$ is the modal mechanical response for the series connection of the piezoelectric layers. The eigenfunctions $U_r(x)$ are given by:

$$U_r(x) = C_r\left\{\cos\left(\frac{\lambda_r}{L_S}x\right) - \cosh\left(\frac{\lambda_r}{L_S}x\right) + \alpha_r\left[\sin\left(\frac{\lambda_r}{L_S}x\right) - \sinh\left(\frac{\lambda_r}{L_S}x\right)\right]\right\} \tag{5}$$

where L_S is the length of the substructure and

$$\alpha_r = \frac{\sin(\lambda_r) - \sinh(\lambda_r) + \dfrac{\lambda_r M_t}{mL_S}\left[\cos(\lambda_r) - \cosh(\lambda_r)\right]}{\cos(\lambda_r) - \cosh(\lambda_r) - \dfrac{\lambda_r M_t}{mL_S}\left[\sin(\lambda_r) - \sinh(\lambda_r)\right]} \tag{6}$$

where M_t is the mass of the tip mass, m is the mass per unit length of the beam which can be written as

$$m = \frac{\rho_S L_S b_S h_S + 2\rho_p (L_2 - L_1) b_p h_p}{L_S} \tag{7}$$

where ρ_S is the substructure mass density, ρ_p is the piezo mass density, L_1 is the initial position of the piezo layer, L_2 is the final position of the piezo layer, b_S is the width of the piezo layer and h_S is the thickness of the substructure. In this study, the initial position of the piezo layer is $L_1 = 0$.

The eigenvalues λ_r can be obtained through the characteristic frequency equation, given as

$$\begin{aligned} &1 + \cos(\lambda)\cosh(\lambda) + \frac{\lambda M_t}{ML_S}\left[\cos(\lambda)\sinh(\lambda) - \sin(\lambda)\cosh(\lambda)\right] \\ &- \frac{\lambda^3 I_t}{mL_S^3}\left[\cosh(\lambda)\sin(\lambda) + \sinh(\lambda)\cos(\lambda)\right] + \frac{\lambda^4 M_t I_t}{m^2 L_S^4}\left[1 - \cos(\lambda)\cosh(\lambda)\right] = 0 \end{aligned} \tag{8}$$

where I_t is the tip mass rotary inertia.

The mechanical equation of motion in modal coordinates can be obtained as

$$\frac{d^2\eta_r^{ser}(t)}{dt^2} + 2\zeta_r\omega_r\frac{d\eta_r^{ser}(t)}{dt} + \omega_r^2\eta_r^{ser}(t) + \chi_r^{ser}v_{ser}(t) = N_r(t) \tag{9}$$

where ζ_r is the modal damping ratio of the r^{th} vibration mode that is given according to the following expression

$$\zeta_r = \frac{c_r}{2\omega_r} = \frac{1}{2\omega_r}\left(c_S I\frac{\omega_r^2}{(YI)} + \frac{c_a}{m}\right) = \frac{c_S I\omega_r}{2(YI)} + \frac{c_a}{2m\omega_r} \tag{10}$$

where c_s stands for the kelvin-Voigt (strain rate) damping coefficient and c_a reflects the contribution of viscous effects (air damping) to the modal damping ratio. The determination of these coefficients is generally difficult and the most

common way to treat damping is to get an equivalent ζ_r from actual experimental data by employing standard modal testing techniques. *This last approach was used in the present study and the* ***constant*** *value of* ζ_r *= 0.0027 was employed for all numerical simulations*. Additional considerations on the damping mechanism and its influence on the optimization process will be further provided in Section 4.0.

Following the description of the modal model for the harvester (Equation (9)), the modal electromechanical coupling term is given as

$$\chi_r^{ser} = \vartheta_{ser} \left. \frac{dU_r(x)}{dx} \right|_{x=L_p} \tag{11}$$

and the piezoelectric coupling term ϑ_{ser} is given by

$$\vartheta_{ser} = \frac{Y_p d_{31} b_p}{2h_p} \left[\frac{h_S^2}{4} - \left(h_p + \frac{h_S}{2} \right)^2 \right] \tag{12}$$

Y_p is the Young's modulus of the piezo, d_{31} is the piezoelectric constant and h_S is the thickness of the substructure.

The undamped natural frequency, ω_r, for the the r^{th} vibration mode is given by

$$\omega_r = \lambda_r^2 \sqrt{\frac{(YI)}{mL_S^4}} \tag{13}$$

The bending stiffness (YI) can be written as

$$(YI) = (YI)_S \frac{L_1}{L_S} + (YI)_B \frac{(L_2 - L_1)}{L_S} + (YI)_S \frac{(L_S - L_2)}{L_S} \tag{14}$$

where $(YI)_S$ is the bending stiffness of the beam without the piezo layer (that corresponds to the beam at the interval $L_2 < x < L_S$) and the component $(YI)_B$ is the bending stiffness of the totally bimorph beam (that corresponds to the beam at the interval $L_1 \le x \le L_2$). The $(YI)_S$ and $(YI)_B$ terms are given by

$$\begin{aligned} (YI)_S &= Y_S I_S = \frac{Y_S b_S h_S^3}{12} \\ (YI)_B &= \frac{2}{3} \left\{ Y_S b_S \frac{h_S^3}{8} + Y_p b_p \left[\left(h_p + \frac{h_S}{2} \right)^3 - \frac{h_S^3}{8} \right] \right\} \end{aligned} \tag{15}$$

If the translational components of the base displacement, given by Eq. (2) is harmonic of the form $g(t) = Y_0 e^{j\omega t}$, where Y_0 is the translational displacement amplitude of the base, ω is the excitation frequency and $j = \sqrt{-1}$, then, the modal forcing function given by Eq. (8) is harmonic and can be expressed as

$$N_r(t) = \left(-\sigma_r \omega^2 Y_0 \right) e^{j\omega t} \tag{16}$$

where

$$\sigma_r = -\left(m - \frac{jc_a}{\omega} \right) \int_o^{L_S} U_r(x) dx + M_t U_r(L_S) \tag{17}$$

c_a is the air damping coefficient and it corresponds to the influence of the air in the external excitation. In this study, the influence of the air in the external excitation will be neglected. The steady state voltage response, $v_{ser}(t)$, is assumed to be harmonic and can be written in terms of the translational base acceleration as

$$v_{ser}(t) = \alpha_{ser}(\omega)\left(-\omega^2 Y_0\right) e^{j\omega t} \tag{18}$$

where the FRF that relates the voltage output to translational base acceleration, $\alpha_{ser}(\omega)$, is given by

$$\alpha_{ser}(\omega) = \frac{\sum_{r=1}^{\infty} \frac{j\omega\kappa_r \sigma_r}{\left(\omega_r^2 - \omega^2 + j2\zeta_r \omega\omega_r\right)}}{\frac{1}{R_l} + j\omega\frac{C_p}{2} + \sum_{r=1}^{\infty} \frac{j\omega\kappa_r \chi_r^{ser}}{\left(\omega_r^2 - \omega^2 + j2\zeta_r \omega\omega_r\right)}} \tag{19}$$

The modal coupling term κ_r is then

$$\kappa_r = -\frac{Y_p d_{31} h_{pc} b_p}{2} \left.\frac{dU_r(x)}{dx}\right|_{x=L_p} \tag{20}$$

where h_{pc} is the distance between the neutral axis and the center of the piezoceramic layer.

In order to obtain the maximum electrical responses it is preferable to excite a given harvester at its fundamental resonance frequency (Erturk et al. 2009b). This is the modal excitation in the first vibration mode, which corresponds to $r = 1$ in Eq. (19).

3. DEFINITION OF THE OPTIMIZATION PROBLEM

In this study, the energy harvesting optimization problem consists in obtaining the maximum power through the peak voltage in the voltage FRF. The parameters to be optimized are: the length of the piezoelectric element, L_p, the length of the substructure, L_S, and the height of the tip mass, h_t. Two different optimization techniques were used: the classical Sequential Quadratic Program (SQP) technique and the Extensive Search (ES) technique.

The optimization problem is a minimization problem and can be stated as

Find $X = \begin{Bmatrix} L_S \\ h_t \\ L_p \end{Bmatrix}$ which minimizes $f(X)$, subject to the constraints

$$\begin{aligned}
&g_1(X): \omega_r \geq \omega_{\min} = 2\pi f_{\min} \\
&g_2(X): \omega_r \leq \omega_{\max} = 2\pi f_{\max} \\
&g_3(X): L_S \geq LL_S \\
&g_4(X): L_S \leq UL_S \\
&g_5(X): h_t \geq Lh_t \\
&g_6(X): h_t \leq Uh_t \\
&g_7(X): L_p \geq LL_p \\
&g_8(X): L_p \leq L_s
\end{aligned} \tag{21}$$

where the fixed terms LL_S (lower length of substructure), UL_S (upper length of substructure), Lh_t (lower height of tip mass), Uh_t (upper height of tip mass) and LL_p (lower length of piezo layer) are the pre-assigned parameters and their values are set according to the design characteristics. X is a vector containing the design variables. The objective function $f(X)$ is the inverse of the voltage FRF for series connection of the piezo layers (given by Eq. (19)).

The constraints g_1 to g_8 depend on the design parameters and the optimization problem finds the value that gives the peak voltage through the electromechanical FRFs. In this study, the previously described constraints $g_1(X)$ and

$g_2(X)$ are nonlinear constraints since the modal undamped natural frequency ω_r relates the design variables according to a nonlinear relationship; $g_3(X)$, $g_4(X)$, $g_5(X)$ and $g_6(X)$ are bounds; $g_7(X)$ and $g_8(X)$ are linear constraints, since the design variables are related according to a linear relationship. Further details on the linear and nonlinear relationships among the optimization variables will be provided later.

3.1. Implementation of SQP through software MATLAB®

The SQP is a classical optimization technique and it can be applied in multidimensional constrained nonlinear minimization problems and in the present work it will be implemented using MATLAB® through command "*fmincon*". This built-in routine finds a constrained minimum of a function of several variables according to the following relationships

Find $X = \begin{Bmatrix} x_1 \\ x_2 \\ \vdots \\ x_n \end{Bmatrix}$ which minimizes $f(X)$, subject to the constraints:

$$A * X \le B \, , A_{eq} * X = B_{eq} \tag{22}$$

$$C(X) \le 0 \, , C_{eq}(X) = 0 \tag{23}$$

$$LB \le X \le UB \tag{24}$$

Inequalities given in (22), (23) and (24) refer to linear constraints, nonlinear constraints and bounds respectively. Subscript *eq* refers to equality constraints. A is the matrix for linear inequality constraints, B is the vector for linear inequality constraints, A_{eq} is the matrix for linear equality constraints, B_{eq} is the vector for linear equality constraints, LB is the vector of lower bounds, UB is the vector of upper bounds, $C(x)$ and $C_{eq}(x)$ are functions that return vectors (can be nonlinear functions) and $f(X)$ is the objective function that returns a scalar.

First, it is necessary to define the design variables. Thus, through the definition of the optimization problem,

$$x_1 = L_S \; ; \; x_2 = h_t \; ; \; x_3 = L_p \tag{25}$$

To apply the command for the optimization problem, the constraints g_1 to g_8 (in the form of Eq. (21)) must be rewritten in the form corresponding to the Eqs. (22) to (24).

Thus, the constraints g_1 and g_2 can be rewritten as

$$\begin{aligned} g_1(X) &: -\omega_r + 2\pi f_{\min} \le 0 \\ g_2(X) &: \omega_r - 2\pi f_{\max} \le 0 \end{aligned} \tag{26}$$

Then, the matrix $C_{2\times 1}$ in Eq. (23) can be given as

$$C = \begin{bmatrix} -\omega_r + 2\pi f_{\min} \\ \omega_r - 2\pi f_{\max} \end{bmatrix} \tag{27}$$

where ω_r is a nonlinear function relating the design variables according to Eq. (13). The terms λ_r and (YI) are functions that also relate the design variables (Eqs. (8) and (14)).

The constraints g_3 to g_6 can be associated to Eq. (24) that defines a set of lower and upper bounds on the design variables, so that a solution is found in the range $LB \le X \le UB$, where

$$LB = \begin{bmatrix} LL_S \\ Lh_t \end{bmatrix} , UB = \begin{bmatrix} UL_S \\ Uh_t \end{bmatrix} \tag{28}$$

It is possible to note that only the design variables x_1 and x_2 are related through the bounds.

The constraints g_7 and g_8 can be rewritten as

$$\begin{aligned} g_7(X) &: -L_p \le -LL_p \\ g_8(X) &: -L_s + L_p \le 0 \end{aligned} \tag{29}$$

Since both constraints are linear, they can be formulated as the matrix inequality given by Eq. (22) where

$$A = \begin{bmatrix} 0 & 0 & -1 \\ -1 & 0 & 1 \end{bmatrix}, B = \begin{bmatrix} -LL_p \\ 0 \end{bmatrix} \tag{30}$$

Hence the second column of matrix A is null, the design variable x_2 is not related in the linear constraints.

After all the matrices of Eqs. (22) to (24) are defined, the command "*fmincon*" can be used like a minimization problem as

$$X = \text{fmincon}(f(X), X_0, A, B, A_{eq}, B_{eq}, LB, UB, \text{NONCON}, \text{OPTIONS}) \tag{31}$$

where the vector X_0 corresponds to the initial guess at the solution, the nonlinear constraint function, NONLCON, accepts X and returns the vectors C and C_{eq}, representing the nonlinear inequalities and equalities respectively. The MATLAB® code given by Eq. (31) minimizes $f(X)$ with the optimization options specified in the structure OPTIONS. Hence there are no equality constraints, the matrices A_{eq}, B_{eq} and C_{eq} must be set as $A_{eq} = [\,]$, $B_{eq} = [\,]$ and $C_{eq} = [\,]$.

3.2 Implementation of the Extensive Search (ES) optimization technique

The ES method is based on the variation of harvester's parameters for obtaining the maximum power through FRF results. For implementing the method, it is necessary to set a project natural frequency range for the harvester device, that is, to set a minimum and a maximum project frequency. The natural frequency of the harvester device must be inside this frequency range. The choice of the project natural frequency range depends on the environmental vibrations corresponding to the structure, machines, equipments in which it is wish to harvest energy from the lost vibrations.

After the maximum and minimum project frequency were chosen, the next step is setting the length of the substructure (beam), L_S, and the height of the tip mass, h_t, for getting the harvesting natural frequency inside the project frequency range. Setting the height of the tip mass is the same as setting the mass of the tip mass. The width of tip mass is the same as the piezo and substructure. The height and the length of tip mass are the same, given by h_t.

The procedure of finding/getting L_S and h_t values is the following:

1st step: the length of the beam/substructure is varied from an initial length up to a final length, for example, varying from 0.1 to 0.3 m in 0.02 in 0.02 m. These values are set by the user and can vary according to the project, assuming any value;

2nd step: for each L_S of the previous step, the h_t value is varied from an initial value up to a final value, for example, varying from 0.004 to 0.020 m in 0.002 in 0.002 m.

It is important to notice that the thickness of the piezo and substructure do not change in each step, but these parameters might assume any value according to the project needs.

For all possible configurations obtained in the steps, one, none, or several configurations of L_S and h_t can be used to get the harvesting natural frequency inside the project frequency range. The best configuration to be used depends on the project features, as for instance, the location where the harvester will be installed, the available materials, costs etc.

If none configurations for L_S and h_t was obtained, there is the necessity of changing some harvester parameters. One or more than one parameters can be changed at the same time. If the frequency range can not be changed, one solution is to change the geometric and physical properties of the substructure or piezo. Some possible parameters available to be changed are basically: material, width, thickness of the substructure or piezo. The influence of the piezo in the choice of L_S and h_t will be discussed later.

Now, if several configurations of L_S and h_t were obtained, the procedure for getting the best configuration depends strongly on the project geometric characteristics. This fact is interesting due to the difficult in building harvesting devices whose first natural frequency is the same as the host structure. Usually, the environmental vibrations are found to be in the frequency range of 0 to 100Hz.

The influence of the piezo in the L_S and h_t achievement is the following: before varying the length of the piezo in order to obtain the maximum FRF peak voltage, one certain length is necessary to be set for getting the project natural frequency. This procedure requires a certain attention because the length of the piezo is also related to the natural frequency of the harvesting device. Thus, the best is to consider a totally bimorph structure for each step of L_S, that is, for each step for L_S, the L_p parameter assumes the same value as L_S. If several combinations for L_S and h_t are found, the best combination is that one in which L_S is maximum and, for this value of L_S, h_t is minimum. This choice is justified since when L_p is varied from 0 to L_S, almost all of the corresponding natural frequencies will fall within the project frequency range.

After obtaining the convenient L_S and h_t values, the relation between the peak voltage in the FRF and the length of the piezo is gotten. In this procedure, it is possible to observe that, for certain L_p value, the peak voltage is maximum. This L_p value is then the optimum value. In some cases, more than one optimum L_p value can be obtained at the same analysis. In this case, if the peaks voltage were approximately the same, it is convenient to use the lowest L_p value because of the harvester design costs attributed to the piezo costs. However, the parameter cost is not analyzed in this study. The choice of the optimum L_p value is not trivial and in some cases, it can involve a more detailed study of the harvester features/design.

4. RESULTS AND DISCUSSION

The optimization procedure was numerically applied in an energy harvesting system represented by a cantilever beam with tip mass excited from base acceleration. The minimum and maximum project frequency was set to be 10 and 20 Hz respectively. The geometric and material parameters used in the modeling are shown in Tab. 1. The permittivity at constant strain is given in terms of permittivity of free space, $\varepsilon_0 = 8.854$ pF/m. The resistive load, R_l, used in the circuit was 100 kΩ.

Table 1. Geometric and material parameters used in the energy harvesting system modeling.

	Structure/Structural Part		
Geometric Parameters	Substructure (Spring Steel)	Piezo. (PZT-5A)	Tip Mass
Length, L (m)	50.8 – 203.2	0 – L_S	6 – 20
Width, b (m)	0.0254	0.0254	0.0254
Thickness, h (m)	0.00254	0.00254	0.006 – 0.020
Material Parameters			
Mass density, ρ (kg/m^3)	7860	7800	7860
Young's Modulus, Y (GPa)	207	67	207
Piezo. Constant, d_{31}, (pm/V)	---	-190	---
Permittivity, $\bar{\varepsilon}_{33}$, (F/m)	---	830 ε_0	---

The analysis of the results starts with the "Extensive Search" method. Figure (3a) shows all the combinations for L_S and h_t gotten. It's possible to observe that there are many combinations in which the natural frequency is inside the project frequency range. The best combination was explained in the previously section. Thus, the L_S and h_t values are 0.1969 m and 0.006 m respectively. For these values, the length of the piezoelectric layers was varied from 0 to L_S and the relation between L_p and the peak voltage is shown in Fig. (3b). In this figure, it is possible to observe that the best configuration to the harvester is not a totally bimorph cantilever. The L_p optimum obtained was 0.1788 m. Figure (3b)

also illustrates the differences in the peak voltages when a constant modal damping ratio is used as opposed to a variable value for ζ_r as given by Eq. (10) (assuming a constant value for c_s and $c_a = 0$). It is seen that a constant modal damping ratio leads to higher values of the peak voltages (dashed line) as compared to a variable damping ratio (solid line). This difference affects directly the output electrical power obtained for the harvester since this quantity depends directly on the value of the peak voltage. However, the results for the optimum harvester geometry from the ES technique resulted insensitive to this damping variation since the same results were obtained with either a constant or variable modal damping ratio. Figure (4a) shows how the strain rate modal damping varies with the length of the piezoelectric layer attached to the cantilever beam. Again, the result shown in Fig. (4a) was obtained from Eq. (10) with $c_a = 0$. It is seen that although modal damping varies with the length of the piezoelectric layer, what in principle conflicts with the constant value adopted here, the constant value for the modal damping ratio used ($\zeta_r = 0.027$) corresponds to the case where the piezoelectric material covers the entire beam, and this is in agreement with the result obtained from the experimental analysis where a fully covered bimorph cantilever harvester was tested in order to get the value for the modal damping ratio. Moreover, as previously stated, the optimum value for Lp was 0.1788 m, and for this value the curves in Fig. (3b) are nearly the same.

To verify if the optimum obtained values can be used to generate a harvester system whose natural frequency falls within the project frequency range, the FRFs are plotted to all L_p values generating the surface shown in Fig. (4a). It can be seen that the peaks formed in Fig. (4a) are the same as those shown in Fig. (3b). For a better visualization, Fig. (4b) shows how the natural frequency was affected by the L_p variation. In this figure, it's possible to observe that there are some combinations in which the natural frequency is not inside the frequency range, but for the optimum configuration corresponding to L_p = 0.180 m, the resulting natural frequency is 10.367 Hz (inside the project natural frequency range).

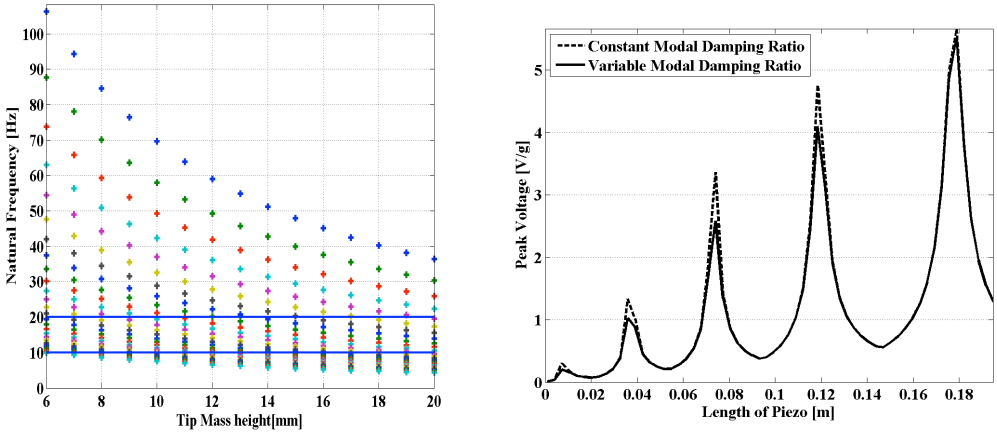

(a) (b)

Figure 3. Influence of L_S and h_t in the harvester natural frequency and (b) influence of L_p in the peak voltage FRF.

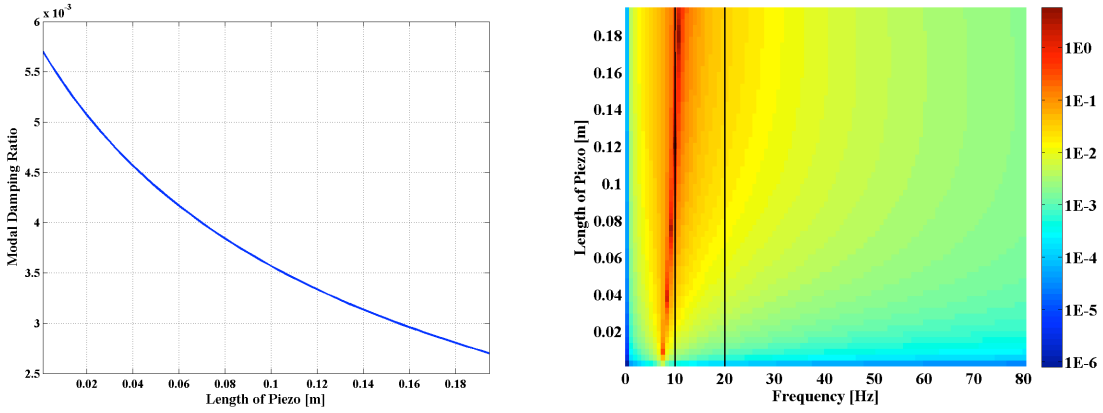

(a) (b)

Figure 4. (a) influence of L_p in the FRF configurations and (b) influence of L_p in the harvester natural frequency

Thus, the design vector obtained for the ES method with dimensions in meters is

$$X_{ES} = \begin{Bmatrix} 0.1969 \\ 0.0060 \\ 0.1788 \end{Bmatrix} \quad (32)\ (31)$$

After applying the command in the software MATLAB® as mentioned in Eq. (32), the optimization procedure using the SQP method resulted in the following design vector with dimensions in meters. The natural frequency gotten was 10.354 Hz, which is also inside the project natural frequency range.

$$X_{SQP} = \begin{Bmatrix} 0.1992 \\ 0.0060 \\ 0.1992 \end{Bmatrix} \quad (33)\ (32)$$

Figure (5a) shows the comparison between the optimum values to each parameter and each presented optimization methods, and Fig. (5b) shows the resulting FRFs generated using the optimum values.

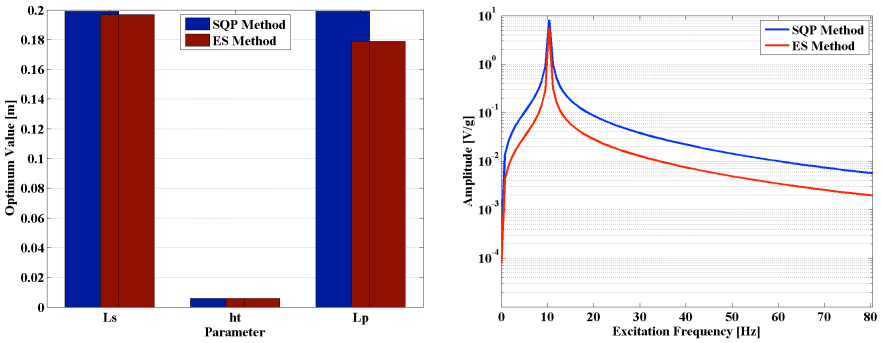

(a) (b)

Figure 5. Comparison between (a) the optimum parameters values and (b) the FRFs for each optimization method.

Inspection of these curves reveal that the natural frequency and the peak voltage for both methods are practically the same, but some parameters for the ES method have lower values.

5. FINAL REMARKS AND CONCLUSIONS

Two different optimization strategies were compared in harvesting electrical energy from a piezoelectric bimorph cantilever beam. In these methods, several parameters were optimized for obtaining the optimum power in piezoelectric energy harvesting from environmental vibrations. The harvester natural frequency was set to fall within a prescribed project natural frequency range, that is, the range in which the environmental vibrations can be. Both ES and SQP methods was capable to solve the proposed optimization problem leading to optimum geometric parameters for the cantilever harvester. The natural frequency and the peak voltage in the FRF were practically the same in both analyses. The ES technique was tested with constant and variable modal damping ratios and the optimization results showed to be insensitive to small variations in damping. However, significant differences were observed in the peak voltages when either constant or variable damping is used what can in principle affect the output electrical power obtained from the harvester. Similar procedure is currently under investigation with the SQP method. Further optimization scenarios are currently under investigation where differences in these techniques should appear according to the parameters to be optimized, in special when variable modal damping ratios are used with the SQP method.

6. ACKNOWLEDGEMENTS

The authors acknowledge the support of Capes and for the financial support and for theirs scholarships. Professor Varoto acknowledges the financial support received from Fapesp (grant # 09/06347-7) during the sabbatical period at Virginia Tech.

7. REFERENCES

Bourisli, R. I. and Al-Ajmi, M. A., 2010, "Optimization of Smart Beams for Maximum Modal Electromechanical Coupling Using Genetic Algorithms", Journal of Intelligent Material Systems and Structures, 21, pp. 907-914.

Dietl, J. M. and Garcia, E., 2010, "Beam Shape Optimization for Power Harvesting", Journal of Intelligent Material Systems and Structures, 21, pp. 633-646.

Erturk, A., Hoffmann, J. and Inman, D.J., 2009a, "A piezomagnetoelastic structure for broadband vibration energy harvesting", Applied Physics Letters, 94, 254102.

Erturk, A and Inman, D.J., 2009b, "An experimentally validated bimorph cantilever model for piezoelectric energy harvesting from base excitations", Smart Materials and Structures, 18, 18pp.

McConnell, K.G. and Varoto, P.S., 2008, "Vibration testing: theory and practice", Ed. John Wiley & Sons, Inc., USA.

Rao, S.S. 2009. "Engineering Optimization: Theory and Practice," Fourth Edition, John Wiley & Sons, Inc.

Renno, J. M., Daqaq, M. F. and Inman, D. J., 2009, "On the optimal energy harvesting from a vibration source", Journal of Sound and Vibration, 320, pp. 386–405.

Stanton, S.C., McGehee, C.C., and Mann, B.P., 2009, "Reversible hysteresis for broadband magnetopiezoelastic energy Harvesting", Applied Physics Letters, 95, 174103.

Wickenheiser, A. M. and Garcia, E., 2010, "Power Optimization of Vibration Energy Harvesters Utilizing Passive and Active Circuits, Journal of Intelligent Material Systems and Structures, 21, pp. 1343-1361.

8. RESPONSIBILITY NOTICE

The authors are the only responsible for the printed material included in this paper.